PHYSICAL REVIEW B **91**, 060506(R) (2015)

# Frequency dispersion of nonlinear response of thin superconducting films in the Berezinskii-Kosterlitz-Thouless state

Scott Dietrich, William Mayer, Sean Byrnes, and Sergey Vitkalov*
*Physics Department, City College of the City University of New York, New York, New York 10031, USA*

A. Sergeev
*SUNY Research Foundation, SUNY at Buffalo, Buffalo, New York 14226, USA*

Anthony T. Bollinger and Ivan Božović
*Brookhaven National Laboratory, Upton, New York 11973, USA*

(Received 28 April 2014; revised manuscript received 27 August 2014; published 20 February 2015)

The effects of microwave radiation on the transport properties of atomically thin $La_{2-x}Sr_xCuO_4$ films were studied in the 0.1–13 GHz frequency range. Resistance changes induced by microwaves were investigated at different temperatures near the superconducting transition. The nonlinear response decreases by several orders of magnitude within a few GHz of a cutoff frequency $\nu_{cut} \approx 2$ GHz. Numerical simulations that assume an ac response to follow the dc $V$-$I$ characteristics of the films reproduce well the low-frequency behavior, but fail above $\nu_{cut}$. The results indicate that two-dimensional (2D) superconductivity is resilient against high-frequency microwave radiation, because vortex-antivortex dissociation is dramatically suppressed in 2D superconducting condensates oscillating at high frequencies.

DOI: 10.1103/PhysRevB.91.060506 PACS number(s): 74.25.N−, 74.25.F−, 74.72.−h, 74.78.−w

Transport properties of thin superconducting films have attracted much interest due to a fascinating physical phenomenon, the Berezinskii-Kosterlitz-Thouless (BKT) transition, predicted to occur at the critical temperature $T_c$ lower than the temperature of the superconducting transition in bulk samples [1–4]. The BKT phase transition originates from long-range (logarithmic) interactions between vortex excitations in a two-dimensional (2D) superconducting condensate. Below $T_c$, the dominant thermal excitations are vortex-antivortex (V-AV) pairs. A superconducting current does not move pairs, thus producing no energy dissipation. However, the current can break some of the V-AV pairs, generate free vortices, set them in motion via the Lorentz force, and thus make the transport dissipative [5–7]. The induced dissociation of V-AV pairs depends on the current strength and thus results in an extraordinary violation of the Ohm's law. With this motivation, the strong nonlinear response to the electric current in thin superconducting films was investigated extensively [8–11]. Despite significant progress, important many-body and edge effects in the V-AV pair dissociation are still under debate [12,13]. Note that the majority of studies of the nonlinear transport in the BKT regime have in fact been done in the dc domain. How condensate oscillations affect the V-AV dissociation is still unclear. Finally, due to strong phase fluctuations, the BKT phenomena are significantly enhanced in superconducting cuprates, especially in heterostructures with a few superconducting copper oxide layers [14]. Our recent studies of dc nonlinearities in molecular beam epitaxy (MBE)-grown heterostructures show that the vortex nonlinearity in the low resistive state exceeds the heating nonlinearity by up to four orders of magnitude [15].

Here, we present experimental investigations of the nonlinear transport properties of atomically thin $La_{2-x}Sr_xCuO_4$ films, over a broad frequency range from dc to 13 GHz. The experiments indicate a dramatic decrease of the nonlinear response at high drive frequencies, suggesting a significant reduction of the V-AV pair dissociation in the oscillating superconducting condensate.

The experiments were performed on thin $La_{2-x}Sr_xCuO_4$ (LSCO) films synthesized by atomic-layer-by-layer molecular beam epitaxy, providing precise atomically thin layers [16–18]. On the extreme level of control, delta doping in a single $CuO_2$ layer has been demonstrated [17]. Recently a linear ac response of such films in the BKT state has been studied [19,20]. The present samples have three distinct layers. The top and the bottom layers, each 5 unit cells (UC) thick, are made of strongly overdoped ($x = 0.41$) normal metals. Sample A, with a 5 UC thick inner layer of $La_{1.72}Sr_{0.28}CuO_4$, shows the BKT transition at $T_c \approx 7$ K [21]. Sample B, with a 1.5 UC thick inner layer of $La_{1.80}Sr_{0.20}CuO_4$, has $T_c \approx 5$ K. Below we study the nonlinear response of the BKT state at $T > T_c$.

The films were patterned into the shape of Hall-bar devices with the width $W = 200$ $\mu$m and the distance between the voltage contacts $L = 800$ $\mu$m. A direct current $I$ was applied through a pair of current contacts, and the longitudinal dc voltage $V$ was measured between the potential contacts. The sample and a calibrated thermometer were mounted on a cold copper finger in vacuum. The electromagnetic (EM) radiation was guided by a rigid coaxial line and applied to samples, as shown in the upper inset in Fig. 1. A 50 Ω resistor terminates the end of the coax and provides the broadband matching of the EM circuit. The EM power $P$ and amplitude of the microwave voltage $V_\nu$ at the end of the coax were measured *in situ* using the nonselective bolometric response of the 50 Ω resistor [21]. In what follows, the measured nonlinear response is normalized with respect to the calibrated EM power $P$,

*Corresponding author: vitkalov@sci.ccny.cuny.edu

 

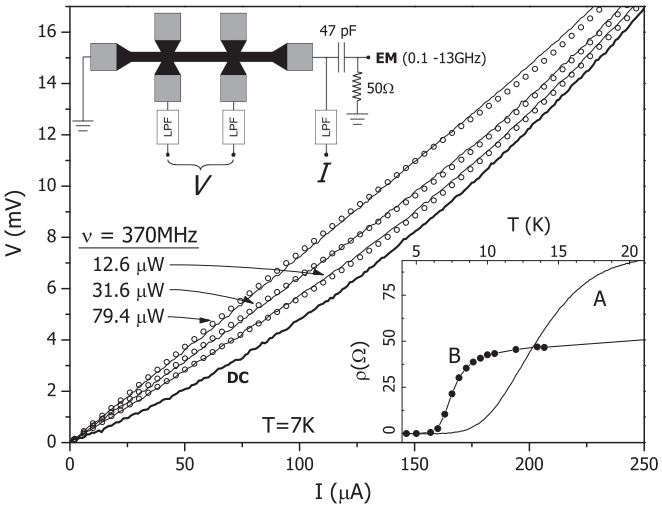


FIG. 1. Dependence of the voltage $V$ on current $I$ at different EM powers applied to a 50 Ω resistor at frequency $\nu = 370$ MHz. The thick solid line represents the dc response with no radiation applied. The open circles are the results of numerical simulations of the effect of EM radiation on a $V$-$I$ curve computed at the same power, for the contact resistance $R_c = 210 \pm 30$ Ω in series with sample B at $T = 7$ K. Upper inset: A schematic of a dc circuit isolated from EM circuitry by a capacitor $C = 47$ pF and three low-pass filters (LPF, $\nu < 100$ MHz). The lower inset shows sheet resistance per square as a function of temperature.

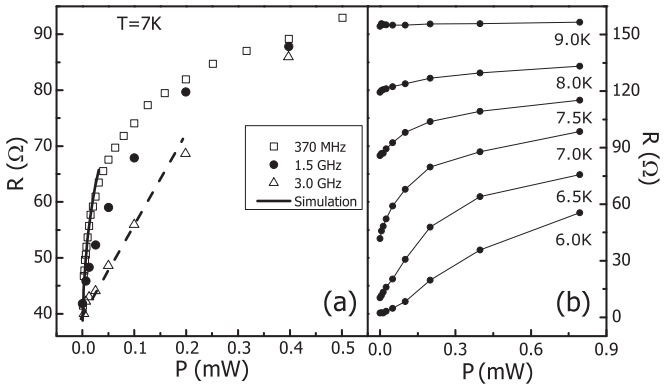


FIG. 2. (a) Dependence of resistance on radiation power shows strikingly different behavior at low frequency (370 MHz) and high frequencies. At frequency 3 GHz the power has been linearly scaled down by a factor of 2 to emphasize a functional difference in the response to EM radiation. The thick solid line is the numerical simulation at contact resistance $R_c = 210$ Ω. The dashed line presents an expected dependence at a small power. (b) Power dependence of resistance at different temperatures, as labeled. $\nu = 1.5$ GHz. Sample B.

which takes into account all the effects of EM transmission (reflection) to (from) the sample stage.

Figure 1 shows the dependence of the voltage $V$ on the current $I$ taken at different powers $P$ of a low-frequency radiation. The thick solid line presents the $V$-$I$ dependence with no radiation applied. The EM radiation increases the resistance, as shown by thin solid lines. To evaluate numerically the radiation effect, the electrical connection (coupling) between the coax and the sample was approximated by a high-frequency contact resistance $R_c$, which determines the total voltage $V_S(t)$ and current $I_S(t)$ applied to the sample, assuming that the electromagnetic response follows the dc nonlinear $V$-$I$ dependence [21]. The time averaged $\langle V_S(t)\rangle$ and $\langle I_S(t)\rangle$ are denoted by the open circles in Fig. 1. The resistance $R_c$ was used as the single fitting parameter for each computed curve, providing a good agreement between the low-frequency experiments and the simulations.

At small currents, both the experiment and the simulations display a linear relation between the current $I$ and voltage $V$—Ohm's law. Figure 2(b) presents the dependence of the ohmic resistance on microwave (MW) power ($\nu = 1.5$ GHz) taken at different temperatures. The solid dots are the slopes of the $V$-$I$ dependencies at small currents. The power dependence varies considerably with the temperature. Close to the superconducting state the microwave-induced resistance variations are strong, whereas near the normal state the variations are weak. The shape of the dependence changes with the temperature. In particular, at $T = 6$ K the dependence looks more linear than at $T = 6.5$ K.

Significant changes in the power dependence are found in the response to microwaves with different frequencies. Figure 2(a) shows the power dependencies of the resistance obtained at frequencies $\nu = 0.37$, 1.5, and 3 GHz. At low frequency $\nu = 0.37$ GHz, the dependence is in a good agreement with the numerical simulation. At high frequencies, the nonlinear response is much weaker and has a different functional form. To highlight the difference, the values of MW power at frequency 3 GHz were scaled down by a factor of 2. A comparison of power dependencies indicates that at a low power the nonlinear response is considerably weaker at a high frequency (3 GHz) than at a low frequency (0.37 GHz). At a high power the strength of the high-frequency nonlinearity is restored.

Figure 3 shows the dependence of radiation-induced variations of the dc voltage $\Delta V$ on dc bias $I$ taken at different frequencies and power levels, as labeled. At small currents, the response is linear, indicating no observable ac rectification in the device. The left panel demonstrates the effect of the low-frequency radiation ($\nu = 0.575$ GHz) on the resistance. All three curves are in very good agreement with the ones obtained by numerical simulations for the same radiation powers [21]. The simulations replicate all the details of the experiments, including the shift of the observed maximum with increased power using the single fitting parameter $R_c = 63 \pm 2\,\Omega$. The right panel shows the effect of the high-frequency ($\nu = 3.4$ GHz) radiation. One can see that the high-frequency response does not follow the dc $V$-$I$ curve and cannot be explained by a reduction (rescaling) of the MW current.

At small currents, the linear part of the voltage variations $\Delta V(I) \sim I$ is related to the change in the ohmic resistance, $\Delta R = R(P) - R(0) = \Delta V(I)/I$. Figure 4 displays the behavior of the resistance variation $\Delta R$ with the power at different frequencies. At a small power, the induced resistance variations are proportional to the power. At higher powers, the dependence is weaker. At higher frequencies, the transition to weak power dependence occurs at a higher power. At the highest power levels all dependencies converge [see Fig. 2(a)].

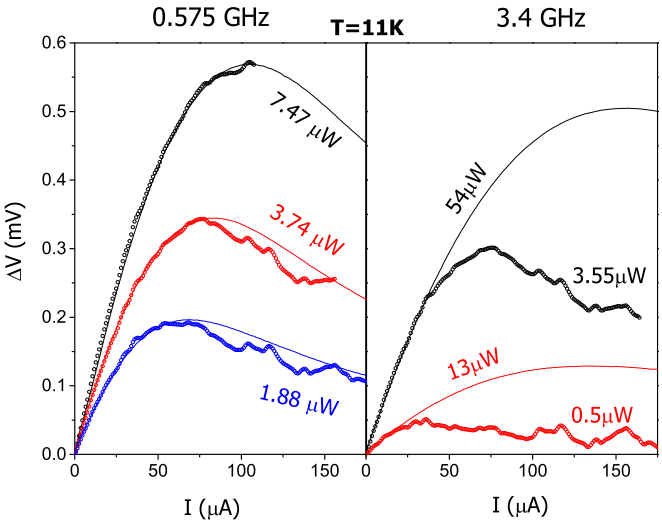


FIG. 3. (Color online) The change in voltage $\Delta V = V(P) - V(0)$ due to applied EM radiation as a function of the dc bias $I$ at different microwave powers, as labeled. The solid lines are experimental data; the open circles present numerical simulations at $R_c = 63 \pm 2\ \Omega$. A comparison of the left and right panels shows the agreement between experiment and simulation at low frequencies, but a serious disparity at high frequencies. Sample A.

An analysis indicates several distinct features of the dc nonlinear response presented in Fig. 1. At small currents the $V$-$I$ dependence is well approximated by a combination of linear and cubic terms [15]. The dependence is presented below,

$$V = R_0 I + \gamma I^3, \tag{1}$$

where $R_0$ is the Ohmic resistance, and the coefficient $\gamma$ is a constant. The high-current behavior is in agreement with the one expected within the BKT scenario, $V \sim I^{\alpha}$ [5,9,10]. The exponent $\alpha(T)$ decreases from 8 to 1 as the temperature

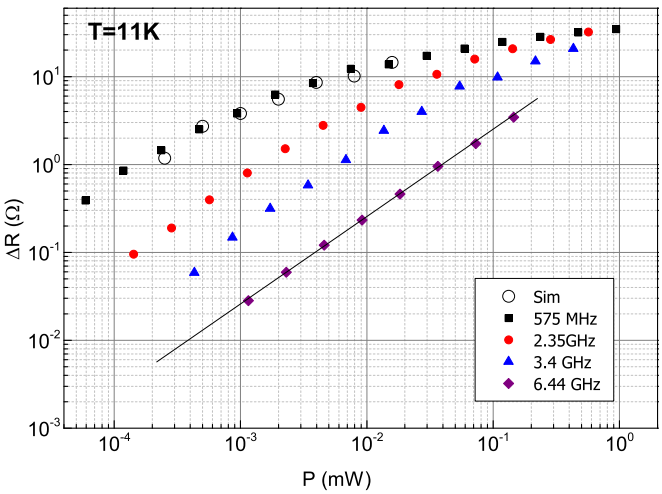


FIG. 4. (Color online) The power dependence of radiation-induced resistance variations $\Delta R = R(P) - R(0) = \Delta V/I$ obtained at small dc biases $\Delta V \sim I$ (see Fig. 3). The solid line is the dependence $\Delta R \sim P$ expected for small power $P$. Open circles are numerical simulations at $R_c = 62\ \Omega$. Sample A.

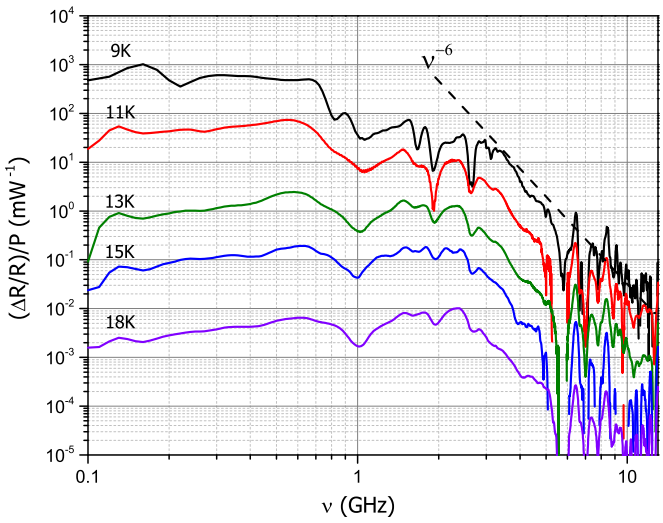


FIG. 5. (Color online) Frequency dependence of the relative variations of the resistance $\Delta R/R$ normalized by applied power $P$ at different temperatures, as labeled. The dashed line is an approximation of the nonlinear response between 3 and 6 GHz. Sample A.

increases, indicating a BKT transition at $\alpha(T_c) = 3$ [21]. In accordance with Eq. (1) at small ac currents $I_\nu(t)$, the voltage variations $\Delta V(I) = \langle V(I + I_\nu(t))\rangle - V(I) \approx 3I\langle I_\nu(t)^2\rangle$ are proportional to the dc bias $I$, which agrees with Fig. 3, and are proportional to the rf power $P \sim I_\nu^2$, which agrees with Fig. 4. The decrease of the nonlinear response shown in Fig. 3 at high dc biases and the transition to a weaker power dependence presented in Fig. 4 are the results of the high current response $V \sim I^{\alpha}$ at $\alpha < 2$.

Figure 5 presents the frequency dependence of the nonlinear response, taken at different temperatures and small powers $P$. At low temperatures, $9\ \mathrm{K} \leqslant T \leqslant 11\ \mathrm{K}$, the response decreases by three to four orders of magnitude, as the frequency increases above a few GHz. This is in a good agreement with the reduction of the dc nonlinearity by three to four orders of magnitude observed between the regimes of V-AV depairing at 10 K and electron heating in the normal state [see Fig. 3(b) in Ref. [15]].

To be sure that the observed effect is not related to a strong decrease in the microwave coupling, we have evaluated the MW current through samples by investigating the MW reflection in the same setup [21]. These studies indicate some frequency dispersion in the MW current. However, the dispersion is nearly uniform and significantly smaller (a variation by a factor of 3–4) than the observed reduction of the nonlinear response by three to four orders of magnitude. Independent measurements of MW voltage, current, and the nonlinear response in several samples allow us to conclude that the observed reduction of the nonlinearity is of a fundamental nature.

Since the reduction is strong, we associate it with the frequency suppression of the dominant mechanism in BKT regime—the current-induced V-AV pair dissociation. If in the course of high-frequency oscillation the distance between the vortex and antivortex within a pair does not exceed a critical distance $l_c$, then the pair can survive. At higher power, the

amplitude of the V-AV oscillations may exceed the critical distance $l_c$, making the response similar to the one obtained at low frequency. It corresponds to Figs. 2(a) and 4.

An analysis of the oscillating vortex motion inside a V-AV pair in the presence of dc depairing current shows rich physics, analogous to the Kapitza pendulum with a vibrating pivot point [22]. Position $x_v$ of a vortex with the mass $M$ moving in a medium with the viscosity $\eta$ under the effect of a time-dependent external potential $U(r,t)$ is given by

$$M\frac{d^2x_v}{dt^2}+\eta\frac{dx_v}{dt}=-\frac{\partial U(r,t)}{\partial r}. \quad (2)$$

The potential $U$ is a sum of the V-AV interaction and a potential of Lorentz force [7], $U(r,t)=2q_0^2\ln(r/\xi)-q_0J_s(t)r$, where $\xi$ is a size of the vortex core and $q_0^2=\pi n_s\hbar^2/4m$, where $n_s$ and $2m$ are density and the mass of the superconducting carriers. We express the supercurrent density $J_s=J_{\rm dc}+J_\omega$ as a sum of the dc bias and current oscillations $J_\omega$ at angular frequency $\omega=2\pi\nu$. An analysis of the ac vortex motion for critical pairs near the saddle point of the potential ($\partial U/\partial r\approx 0$) shows a reduction of the vortex displacement at high frequencies, $x_v^{\rm ac}\approx q_0J_\omega/(-M\omega^2+i\omega\eta)$. Moreover, at $\omega>\omega_c=\eta/M$, the ac depairing is strongly suppressed due to the phase shift between the vortex displacement and the barrier height. At the moments when the potential $U(t)$ reaches a minimum, the displacement is the smallest, thus preventing the V-AV dissociation. Finally, at high frequencies a nonlinear analysis [22] of Eq. (2) indicates an effective attractive force inside the pair, which is proportional to the square of the vortex displacements, $\delta F_{\rm eff}\sim\frac{\partial^3U}{\partial r^3}\langle[x_v^{\rm ac}(t)]^2\rangle\sim\frac{\langle(x_v^{\rm ac})^2\rangle}{r^3}$. These effects reduce the pair dissociation at high driving frequencies. Although the origin of the cutoff frequency $\nu_{\rm cut}$ requires further research, we note that an evaluation of the frequency $\nu_c=\eta/(2\pi M)$ is in a good agreement with our data. Using the Stephen-Bardeen viscosity [23] and considering the vortex mass $M$ as a total mass of electrons in the core [24], we get the characteristic frequency of $\nu_c=2$ GHz at the core radius of 8 nm, which is approximately two times bigger than the superconducting coherence length $\xi$. The above analysis points toward the crucial importance of the displacement-force phase relations in the nonlinear ac response of the bulk BKT state, supporting substantially the fundamental origin of the observed phenomenon.

In summary, a strong nonlinear response to low-frequency radiation is observed in atomically thin superconducting films, in the BKT state. The response decreases by several decades within a few GHz above the cutoff frequency $\nu_{\rm cut}\approx 2$ GHz. This indicates that 2D superconductivity is quite resilient to the high-frequency radiation because of a strong reduction of the vortex-antivortex dissociation in oscillating 2D superconducting systems. This general conclusion is in agreement with the results of the linear response studies of the BKT state in thin disordered films of traditional superconductors. In particular, detailed investigations of the conductivity in the range 9–120 GHz show only frequency-dependent Drude absorption without any measurable dissipation due to vortex-antivortex dissociation [25].

Sample synthesis by ALL-MBE and characterization (I.B.) and device fabrication (A.T.B.) were supported by the U.S. Department of Energy, Basic Energy Sciences, Materials Sciences and Engineering Division. Work at CCNY and SUNY was supported by National Science Foundation, Division of Electrical, Communications and Cyber Systems (ECCS-1128459).

[1] V. L. Berezinskii, Sov. Phys.-JETP **34**, 610 (1972).
[2] J. M. Kosterlitz and D. J. Thouless, J. Phys. C **6**, 1181 (1973).
[3] J. M. Kosterlitz and D. J. Thouless, *Progress in Low Temperature Physics* (Elsevier, Amsterdam, 1978), Vol. 7, Part 2, pp. 371-433.
[4] *40 Years of Berezinskii-Kosterlitz-Thouless Theory*, edited by J. V. Jose (World Scientific, Singapore, 2013).
[5] B. I. Halperin and D. R. Nelson, J. Low Temp. Phys. **36**, 599 (1979).
[6] B. A. Huberman, R. J. Myerson, and S. Doniach, Phys. Rev. Lett. **40**, 780 (1978).
[7] V. Ambegaokar, B. I. Halperin, D. R. Nelson, and E. D. Siggia, Phys. Rev. B **21**, 1806 (1980).
[8] K. Epstein, A. M. Goldman, and A. M. Kadin, Phys. Rev. Lett. **47**, 534 (1981).
[9] A. M. Kadin, K. Epstein, and A. M. Goldman, Phys. Rev. B **27**, 6691 (1983).
[10] A. T. Fiory, A. F. Hebard, and W. I. Glaberson, Phys. Rev. B **28**, 5075 (1983).
[11] A. M. Goldman, in *40 Years of Berezinskii-Kosterlitz-Thouless Theory* (Ref. [4]), pp. 135–160.
[12] A. Gurevich and V. M. Vinokur, Phys. Rev. Lett. **100**, 227007 (2008).
[13] V. G. Kogan, Phys. Rev. B **75**, 064514 (2007).
[14] I. Hetel, T. R. Lemberger, and M. Randeria, Nat. Phys. **3**, 700 (2007).
[15] B. Wen, R. Yakobov, S. A. Vitkalov, and A. Sergeev, Appl. Phys. Lett. **103**, 222601 (2013).
[16] A. Gozar, G. Logvenov, L. Fitting Kourkoutis, A. T. Bollinger, L. A. Giannuzzi, D. A. Muller, and I. Bozovic, Nature (London) **455**, 782 (2008).
[17] G. Logvenov, A. Gozar, and I. Bozovic, Science **326**, 699 (2009).
[18] A. T. Bollinger, G. Dubuis, J. Yoon, D. Pavuna, J. Misewich, and I. Božović, Nature (London) **472**, 458 (2011).
[19] V. A. Gasparov and I. Bozovic, Phys. Rev. B **86**, 094523 (2012).
[20] L. S. Bilbro, R. Valdes Aguilar, G. Logvenov, O. Pelleg, I. Bozovic, and N. P. Armitage, Nat. Phys. **7**, 298 (2011).
[21] See Supplemental Material at http://link.aps.org/supplemental/10.1103/PhysRevB.91.060506 for transport in dc domain at BKT transition, details of numeric simulations, bolometric power calibration and microwave coupling to samples.
[22] L. D. Landau and E. M. Lifshitz, *Course of Theoretical Physics: Mechanics*, 3rd ed. (Pergamon, New York, 1976), Vol. 1, p. 93.
[23] M. J. Stephen and J. Bardeen, Phys. Rev. Lett. **14**, 112 (1965).
[24] G. E. Volovik, JETP Lett. **65**, 217 (1997).
[25] R. W. Crane, N. P. Armitage, A. Johansson, G. Sambandamurthy, D. Shahar, and G. Gruner, Phys. Rev. B **75**, 094506 (2007).